Control of P-Glycoprotein Activity by Membrane Cholesterol Amounts and Their Relation to Multidrug Resistance in Human CEM Leukemia Cells†

Landry Gayet,‡ Guila Dayan,‡ Stéphane Barakat,‡ Stéphane Labialle,‡ Mickaël Michaud,‡ Sylvain Cogne,§ Abdellah Mazane,‡ Anthony W. Coleman,‡ Dominique Rigal,|| and Loris G. Baggetto*,‡

Institut de Biologie et Chimie des Protéines (IBCP UMR5086 CNRS UCBL), 7 Passage du Vercors, F-69367 Lyon Cedex 07, France, Genetic Research Instrumentation France, 4 Impasse de la Croix Blanche, F-95370 Montigny-les-Cormeilles, France, and EFS Lyon, 1 Passage du Vercors, F-69007 Lyon, France

Received June 25, 2004; Revised Manuscript Received October 26, 2004

ABSTRACT: P-glycoprotein (P-gp) is the most well-known ATP-binding cassette (ABC) transporter involved in unidirectional substrate translocation across the membrane lipid bilayer, thereby causing the typical multidrug resistance (MDR) phenotype expressed in many cancers. We observed that in human CEM acute lymphoblastic leukemia cells expressing various degrees of chemoresistance and where P-gp was the sole MDR-related ABC transporter detected, the amount of esterified cholesterol increased linearly with the level of resistance to vinblastine while the amounts of total and free cholesterol increased in a nonlinear way. Membrane cholesterol controlled the ATPase activity of P-gp in a linear manner, whereas the P-gp-induced daunomycin efflux decreased nonlinearly with the depletion of membrane cholesterol. All these elements suggest that cholesterol controls both the ATPase and the drug efflux activities of P-gp. In addition, in CEM cell lines that expressed increasing levels of elevated chemoresistance, the amount of P-gp increases to a plateau value of 40% of the total membrane proteins and remained unvaried while the amount of membrane cholesterol increased with the elevation of the MDR level, strongly suggesting that cholesterol may be directly involved in the typical MDR phenotype. Finally, we showed that the decreased daunomycin efflux by P-gp due to the partial depletion of membrane cholesterol was responsible for the efficient chemosensitization of resistant CEM cells, which could be totally reversed after cholesterol repletion.

The major cause of failure of cancer chemotherapy arises from the development of resistance to anticancer agents. The typical mechanism of resistance to multiple drugs (MDR)[1] consists of expelling drugs out of the cell via transport proteins in such way that the concentration of drugs present in the cell becomes lower than the drug's cytotoxicity threshold. Among the members of the large superfamily of ABC transporters and other transporters that are involved in drug extrusion, P-glycoprotein (or P-gp or ABCB1) has been the most studied protein.

P-gp is reported in chemoresistant cancers, with an incidence for its expression of between 20 and 50% (*1*). It is responsible for the resistance to a broad variety of drugs (*2*, *3*). P-gp is also believed to act as a flippase for translocating a large variety of lipids such as sphingomyelin from the inner to the outer plasma membrane leaflets (*4*).

Finally, P-gp seems correlated to, or even involved in, the esterification of cholesterol, as the level of the latter decreases when the P-gp activity is modulated by certain inhibitors (*5*, *6*). It is thought that P-gp may promote the redistribution of plasma membrane cholesterol toward the endoplasmic reticulum, thereby facilitating cholesterol esterification. The mechanism by which cholesterol is transported toward the endoplasmic reticulum is poorly documented.

Several observations suggest that a total change in the proteolipidic organization of the plasma membranes occurs in resistant cells as compared to sensitive cells. Moreover, this change occurs in several species since it has been observed by electron microscopy in human acute CEM lymphoblastic leukemia and in a murine lymphoid leukemia (*7*, *8*). In addition, it appears that the lipid environment can drastically influence the characteristics of the ATPase activity when P-gp is reconstituted in liposomes of variable lipid composition (*9*). Thus, the increased accumulation of cholesterol in membranes of resistant cells probably has consequences on P-gp activities (*10*, *11*). This is why the depletion of cholesterol in P-gp-dependent vincristine-resistant cells induced the modulation of their level of chemoresistance (*11*). Additionally, it has been shown that P-gp ATPase activity appears to increase when P-gp is reconstituted in cholesterol-containing liposomes (*12*) and that elevated cellular cholesterol levels can markedly increase the P-gp activity in human blood mononuclear cells (*13*). Last, it was shown that P-gp was at least partly localized in

† This work was supported by grants from Ligue contre le Cancer (Comité du Rhône, Comité de la Loire, Comité de la Saône et Loire, Comité National), Retina France, Fondation Mérieux, Fondation pour la Recherche Médicale, Association pour la Recherche contre le Cancer (ARC), and NRC-CNRS program.

* To whom correspondence should be addressed. Tel.: +33 (0)4 72 72 26 35. Fax: +33 (0)4 72 72 26 26. E-mail: lg.baggetto@ibcp.fr.

‡ Institut de Biologie et Chimie des Protéines.

§ Genetic Research Instrumentation France.

|| EFS Lyon.

[1] Abbreviations: ABC transporter, ATP-binding cassette transporter; DRM, detergent-resistant membrane; IR, index of resistance; MDR, multidrug resistance; MβCD, methyl-β-cyclodextrin; P-gp, P-glycoprotein.

10.1021/bi048669w CCC: $30.25
Published on Web 02/23/2005

membrane microdomains that are particularly rich with cholesterol (*14*, *15*).

The work we present here has been carried out on an interesting cell model since its typical MDR phenotype is well-characterized and involves only one ABC transporter (i.e., P-gp). This model is constituted of a sensitive parental cell line delineated in five lines of increasing MDR levels. Although several studies have already addressed certain aspects of the current work (*16*), they were nevertheless accomplished by different groups on different models and in a different context (i.e., in vivo, in vitro, on membranes). The present study was carried out on both entire cells and on bi- or monolayer cell membrane models.

In this paper, we show that cholesterol increases in a nonlinear way with the level of chemoresistance of the human CEM acute lymphoblastic leukemia. However, because of the possible involvement of P-gp in the esterification of cholesterol, we have measured the amounts of esterified cholesterol and observed a linear increase with the levels of chemoresistance. In addition, by using biophysical approaches to study the role of cholesterol in the membrane environment of P-gp, we demonstrate that disruption of the membrane organization due to cholesterol depletion could not be repaired by cholesterol repletion and caused drug retention impairments.

Moreover, we show that membrane cholesterol can modulate the P-gp ATPase activity and that its depletion is responsible for the sensitization of resistant CEM cells to daunomycin, thereby assessing the modulating role of cholesterol on the MDR phenotype. Last, we show that these membrane changes are directly correlated to the level of chemoresistance of the involved cells. Our work clearly highlights the complex effect of cholesterol on the MDR phenotype and opens new insights on the possibility of chemosensitizing resistant cells by the modulation of their membrane cholesterol content.

MATERIALS AND METHODS

Chemicals. Except when indicated, all chemicals were from Sigma-Aldrich (France). Cab-O-Sil grade M-5 silica resin was from Lambert Rivière S. A. (Fontenay-sous-Bois, France).

Cell Culture and Viability. Sensitive (CEM/S) and resistant (CEM/VLB0.45 (resistance index 4483 for vinblastine), CEM/VLB3.6 (resistance index 14 552 for vinblastine), CEM/VLB5 (resistance index 18 793 for vinblastine), CEM/VLB8 (resistance index 22 089 for vinblastine), and CEM/VLB10 (resistance index 42 069 for vinblastine)) human lymphoblastic leukemia CEM cell lines were maintained in RPMI-1640 medium, as previously described (*17*). Resistant indexes were determined as described previously (*18*). All these cell lines were regularly checked for mycoplasma contamination with both MycoTect (Gibco-BRL Life Technologies, France) according to the manufacturer's instructions and by fluorescence staining with Hoechst 33258 (Sigma, France). Cell viability was measured by exclusion of Trypan blue (Sigma, France).

Cholesterol Isolation and Quantification of Total, Esterified, and Free Cholesterol. Cellular cholesterol was extracted with 2-propanol using a modified protocol (*19*); briefly, 6×10^6 cells were washed three times with PBS by centrifugation at 800*g* for 5 min and at 4 °C. Pelleted cells were resuspended in 1 mL of 2-propanol and sonicated for three 30 s periods interrupted by 1 min cooling periods, with a Branson Sonifier 250 using a microprobe. After centrifugation during 5 min at 800*g*, the pellet was used to quantify the proteins. After evaporation of 2-propanol, total cholesterol was measured in the supernatant using a method that was initially designed for serum cholesterol (*20*) and that has been modified for cellular cholesterol (*21*) using the CHOD-PAP kit (Biolabo). Free cholesterol was measured using the same protocol in the absence of cholesterol esterase. Esterified cholesterol was obtained by subtracting free from total cholesterol.

In the case of total cholesterol from plasma membrane extracts, the same procedure was applied using 20 μL of membrane extracts containing about 60 μg of membrane proteins, which gave the membrane cholesterol content.

Cell Depletion and Repletion of Membrane Cholesterol. For cell cholesterol depletion, 0−1.5 mM MβCD were added to 1×10^6 cells cultured in the previously described conditions (*22*).

To inhibit endogenous cholesterol synthesis and recycling, cells were cultured in the presence of 10 mM mevalonate and 1.35 mM lovastatin in the RPMI-1640 medium supplemented with 10% fetal bovine serum (FBS). The latter had previously been heat-inactivated at 56 °C for 30 min and defatted according to refs *23*−*25*. Briefly, 7.5 g of Cab-O-Sil silica resin was added to 250 mL of FBS under constant slow agitation during 48 h at room temperature. FBS was subsequently sterile-filtered and controlled for the absence of cholesterol.

For cell cholesterol enrichment and repletion, cholesterol (6.5 mM final concentrated) dissolved in a 2-propanol/chloroform 2:1 (v/v) mixture was added to the aqueous 66.7 mM MβCD solution previously heated at 80 °C. Upon evaporation of the 2-propanol/chloroform solution mixture, cholesterol progressively associated with MβCD forming a soluble mixture containing 66.7 mM MβCD and 6.5 mM cholesterol. Cholesterol repletion was carried out by adding 0.3 μL of the extemporaneously prepared MβCD/cholesterol complex to 1 mL of cells (10^6 cells) cultured for 4 h at 37 °C.

Isolation of Plasma Membranes. Plasma membranes were prepared by sonication and discontinuous sucrose density gradient ultracentrifugation according to ref *17*. Briefly, 5×10^8 cells were quickly thawed in 1 mL of buffer containing 50 mM Tris-HCl (pH 7.4), 150 mM NaCl, 2 mM EDTA, 2 mM phenylmethanesulfonyl fluoride, 1 μM leupeptin, and 2 μM pepstatin A and were sonicated for three 30 s bursts with 1 min cooling periods between. The melt was loaded onto a discontinuous sucrose gradient consisting of 4 mL of 45%, 3 mL of 31%, and 2 mL of 16% (w/v) sucrose in 10 mM Tris-HCl (pH 7.4) and ultracentrifuged at 4 °C in a swinging bucket SW41Ti rotor (Beckman) for 18 h at 100 000*g*. The P-gp-containing membrane fraction was collected at the 16:31% sucrose interface, diluted to 12 mL with 10 mM Tris-HCl (pH 7.4), and pelleted by ultracentrifugation (100 000*g*, 1 h, 4 °C). For depletion of membrane cholesterol, the 16:31% sucrose interface was diluted to 12 mL with 10 mM Tris-HCl (pH 7.4) and 1.5 mM methyl-β-cyclodextrin, incubated for 1 h at 37 °C, and pelleted by ultracentrifugation (100 000*g*, 1 h, 4 °C, Beckman SW41Ti

rotor). The pellets were suspended in 0.25 M sucrose and 10 mM Tris-HCl (pH 7.4). For repletion assays, pellets were diluted to 12 mL with 0.3 μL/mL MβCD/cholesterol complex in 10 mM Tris-HCl, pH 7.4, and treated as stated previously.

Measurement of P-gp ATPase Activity. The hydrolysis of ATP by P-gp was measured using an NADH fluorimetric assay (*26*). Briefly, the decrease of NADH fluorescence emission at 460 nm was quantitatively recorded at 30 °C by using an SLM Aminco 8000C spectrofluorimeter (SLM Instruments Co.) in 1.5 mL of reaction buffer containing 40 mM Tris-HCl (pH7.4), 6 mM $MgCl_2$, 0.5 mM EDTA, 20 mM DTT, 0.25 mM phosphoenolpyruvate, 26 μM NADH, 1.5 mM ATP, 30 μg/mL pyruvate kinase, 15 μg/mL lactate dehydrogenase, and 1−5 μg of plasma membranes. ATPase activity was assayed after the addition of specific ATPase inhibitor mixture (20 mM NaN_3, 1 mM EGTA, 4 mM ouabain, 1 μg/mL oligomycin) in the assay medium. Values from CEM/S cells were taken as a control.

Protein Separation by Electrophoresis and Immunoblotting. Protein concentration was measured by the Bradford method (*27*) using fatty acid free-bovine serum albumin as a standard.

Proteins (11 μg) from untreated or cholesterol-depleted plasma membranes in 1 μL of buffer containing 62.5 mM Tris, pH 6.8, 2% SDS (w/v), 25% glycerol (v/v), and 0.01% β-mercaptoethanol (w/v) were subjected to electrophoretic migration according to ref *28*. Proteins were stained with Coomassie blue R250.

Proteins from SDS−PAGE were transferred for 1.5 h at 250 mA to a 0.45 μm nitrocellulose membrane (BA85, Schleicher and Schüell) in 12.5 mM Tris-base, pH 8.3, 96 mM glycine, 20% ethanol, and then labeled with the C219 anti-P-gp monoclonal antibodies (Dako, dilution 1/500) for 1 h at room temperature, followed by the secondary alkaline phosphatase-labeled antibody (1:2500) for 1 h, and revealed in the presence of 5-bromo-4-chloro-3-indolyl phosphate and nitro blue tetrazolium chloride for 15 min.

Protein Analysis by Mass Spectrometry. The band of interest was cut out from the gel. In-gel proteins were reduced in 10 mM DDT in 50 mM NH_4HCO_3, 56 °C for 40 min and digested with porcine trypsin (0.5 μg, Grade modified, Promega) in 50 mM NH_4HCO_3 pH 8.3 at 37 °C for 5−6 h. Peptide mass fingerprinting was determined by MALDI-TOF mass spectrometry on a Voyager DE-PRO (Applied Biosystems, France) instrument using α-cyano-4-hydroxycinnamic acid as the matrix. Peptide monoisotopic masses were compared to theoretical masses from the NCBI Sequence Databases using the MASCOT (Matrix Science, UK) search engine software. Typical search parameters were as follows: ±30 ppm of mass tolerance, carbamidomethylation of cystein residues, one missed enzymatic cleavage for trypsin, and methionine residues could be considered in the oxidized form, no restriction was placed on the pI of the protein, and a protein mass range from 10−170 kDa was allowed.

Langmuir Compression Isotherms. The effect of the concentration of P-gp in the membrane on the properties of monolayers prepared from membrane fractions of CEM/S, CEM/VLB0.45, and CEM/VLB10 cells was analyzed by Langmuir compression isotherms (*29*). Monolayers from membrane fractions extracted from P-gp-containing cells were produced and studied using a Lauda Film Balance (Germany) and NIMA (England) setups operating as a Langmuir balance. The subphase was composed of 10 mM phosphate buffer (pH 7.0). To form a monolayer, 10 μL of a solution of membrane fractions (with a protein concentration of 8 mg/mL) was applied onto the thoroughly cleaned surface of the subphase between the movable and the measuring barriers. The monolayer was equilibrated during 30 min and then was compressed at a constant rate of 25 cm^2/min by the movable barrier. Simultaneously, the isotherms of the surface pressure π as functions of the monolayer area A per certain weight of the protein in the monolayer are recorded. The surface pressure increases above zero when a condensed layer forms; hence, the increased surface pressure corresponds to a particular proteolipidic organization of the monolayer.

Intracellular Retention of Daunomycin. After a viability test performed by Trypan blue exclusion, resistant or sensitive cells in an exponential growth phase were suspended in 100 μL of ice-cold PBS and immediately analyzed by flow cytometry using a FACSort flow cytometer with Cellquest software (Becton-Dickinson FACS system, France). For daunomycin retention and anexin V-FLUOS (Roche, France) analysis, the excitation source was an argon ion laser emitting at 488 nm with a 15 mW flux intensity. The respective red and green fluorescence of daunomycin and anexin V-FLUOS was collected through a 585:42 nm and a 530:30 band pass filter (FL2 and FL1, respectively) and measured on a four decade logarithmic scale (8000−10 000 events analyzed for each sample). Daunomycin equilibrium time amounted to 3 h for the CEM cell lines, taking into account its membrane partition coefficient, as we had previously determined (*18*). Aliquots of the same cell batches as those used for the retention assays but in the absence of any drug were withdrawn for testing. To test cholesterol-repleted cells that had been previously cholesterol-depleted, cells were previously washed in PBS and resuspended in the cholesterol repletion medium prior to the addition of 1.9 μM daunomycin.

RNA Isolation and RT-PCR. Total RNA was extracted with the RNAgents Total RNA Isolation System (Promega) according to the manufacturer's instructions.

Reverse transcription was carried out by M-MLV reverse transcriptase (Promega-France).

The PCR semiquantification of *MDR*1 transcripts from CEM/S, CEM/VLB0.45, CEM/VLB3.6, CEM/VLB5, CEM/VLB8, and CEM/VLB10 cells was carried out with the Techne thermalCycler model PHC-3 using the DNA binding SYBR Green I dye for the detection of PCR products. The β-actin gene was used as reference. The forward and reverse specific primer sequences used, the size of the amplified fragment, and the annealing temperature are indicated next for *MDR*1: 5′-AAG TGA TAT CAA TGA TAC AGG GTT C-3′ and 5′-TGT TGC CAT TGA CTG AAA GAA CAT T-3′, 313 bp, 60 °C and for β-actin: 5′-CAG AGC AAG AGA GGC ATC CT-3′ and 5′-ATC ATG TTT GAG ACC TTC AA-3′, 209 bp, 50 °C. Qualitative PCR analysis of *LRP*/*MVP*, *BCRP*, *MRP*1, *MDR*1, and *GAPDH* mRNA transcripts from CEM/S, CEM/VLB0.45, CEM/VLB3.6, CEM/VLB5, CEM/VLB8, and CEM/VLB10 cells was carried out as indicated previously using ethidium bromide to detect PCR products. The forward and reverse specific primer sequences used were GTC CAC CAA ATC CAG AAC CTC and TTT

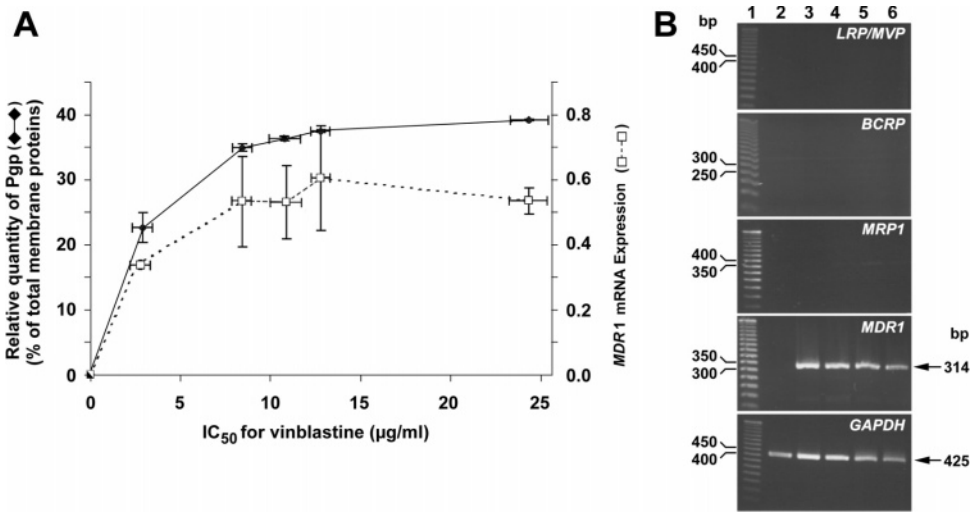

FIGURE 1: Expression of MDR-related proteins. (A) Relative amount of P-gp in membranes of CEM cells (full line) and relative expression of the *MDR*1 mRNA (dotted line), as a function of the IC_{50} for vinblastine. Membranes were prepared from CEM sensitive and resistant cells as indicated in Materials and Methods; proteins were separated by 8% SDS−PAGE. The relative amounts of P-gp in the membranes were obtained by laser scan densitometry of the electrophoretic profiles. The intensity of the detected bands was quantified using the Image QuaNT analysis software and reported relative to the total quantity of membrane proteins detected (left scale). Results are the average of three independent measurements with their standard deviation. Relative expression of *MDR*1 mRNA, which was isolated as indicated in Materials and Methods, was measured from 1.2% agarose gel electrophoresis of RT-PCRs using the β-actin mRNA as internal control. Band intensity was digitized using the STORM 860 laser densitometer and quantified with the Image QuaNT analysis software relative to the β-actin mRNA expression (right scale). Results correspond to an average of three duplicated PCR experiments, which were carried out on three independent reverse transcriptions for each cell line. IC_{50} values are the average of three duplicated independent experiments with their standard deviation. (B) mRNA expression of the main non-P-gp MDR-related genes. RT-PCR amplification of mRNAs from sensitive and resistant CEM cells were carried out with the specific primers mentioned in Materials and Methods and separated on 1.2% agarose gel electrophoresis. Lane 1: molecular weight marker. Ten μL of the reaction mixture from RT-PCRs of *LRP/MVP*, *BCRP*, *MRP*1, *MDR*1, and *GAPDH* mRNAs, as indicated, was deposited in lanes 2−6, which correspond to CEM/S, CEM/VLB0.45, CEM/VLB3.6, CEM/VLB8, and CEM/VLB10 cells, respectively.

GAT GTC ACA GGG CAA GTT for *LRP/MVP* (429 bp product), AGT GGC AGA CTC CAA GGT TG and GCC AAT AAG GTG AGG CTA TCA A for *BCRP* (264 bp product), GTC TTG GTC TTC ATC GCC AT and GAC TGG CAG GGC TAC TTC TAC for *MRP*1 (389 bp product), GTT GCC ATT GAC TGA AAG AAC A and AGA AGT GAT ATC AAT GAT ACA GGG TTC for *MDR*1 (314 bp product), and CCA AAG TTG TCA TGG ATG ACC and GTG GAT ATTGTT GCC ATC AAT G for *GAPDH* (425 bp product).

RESULTS

To study the influence of cholesterol on the activities of P-gp in its membrane microenvironment, the CEM lymphoblastic leukemia cell line, in its sensitive and multidrug resistant derivatives grown in the presence of vinblastine, was used, as previously described (*17*).

P-gp Expression and Membrane Cholesterol Contents Vary as a Nonlinear Function of the Level of MDR in CEM Cell Lines. In our model, both *MDR*1 mRNA and P-gp protein levels increased in a parallel manner as a nonlinear function of the IC_{50} for vinblastine, up to a plateau that was reached with CEM/VLB5 cells ($IC_{50} = 10.9 \pm 2.1$ μg/mL) (Figure 1). The relative maximum amount of P-gp that was produced by CEM/VLB10 cells corresponded to 40% of total membrane proteins (solid trace). Comparable results were obtained for the quantization of *MDR*1 mRNA as a function of the IC_{50} for daunomycin (not shown).

Analysis of membrane extracts by SDS−PAGE followed by an electrotransfer revealed by the C219 anti-P-gp monoclonal antibody shows that P-gp was the highest produced protein in all the resistant CEM cell lines studied (Figure 2). Additionally, analysis of the protein contents in the trypsin-digested band of interest by MALDI-TOF mass spectrometry revealed that the 45 peptides retrieved belonged to P-gp (Table 1). The fragments analyzed covered 37% of the 1280 residues spanning the entire P-gp sequence, and the probability for the analyzed protein to be effectively P-gp exceeded 95%. Moreover, qualitative RT-PCR experiments revealed only *MDR*1 mRNAs while *MRP*1, *LRP/MVP*, or *BCRP* mRNAs were not detected (Figure 1B), strongly suggesting that the typical MDR phenotype of the resistant CEM derivatives is mainly due to the expression of P-gp.

The relationship between cholesterol and the MDR phenotype was addressed by measuring the amount of this lipid in the CEM cell lines of increasing MDR levels. Figure 3 shows that the amount of esterified cholesterol was significantly higher in all resistant CEM cells than in the parental sensitive cells. In addition, the increased amount of total cholesterol was clearly evident with CEM/VLB5 cells and cells with higher MDR levels, and was mainly due to the increased of esterified cholesterol contents.

Comparison of the Proteolipidic Organization of Plasma Membranes from Sensitive and Resistant CEM Cells by the Langmuir Technique. The differences that sensitive and resistant CEM cells displayed in terms of cholesterol amounts led us to address possible different proteolipidic organization of their membranes. We examined this hypothesis by comparing membrane monolayers from sensitive CEM/S and resistant CEM/VLB0.45 and CEM/VLB10 cells using Langmuir compression isotherms. Membrane cholesterol and proteins were measured before each assay.

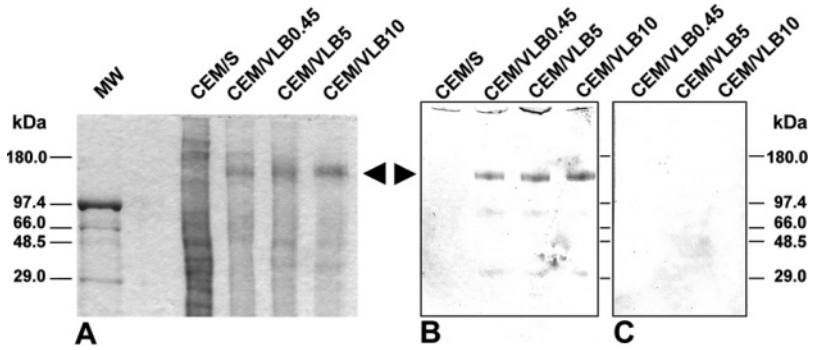

FIGURE 2: Overexpression of P-gp in CEM resistant cells. (A) 8% SDS−PAGE profile of membrane extracts from sensitive CEM/S and resistant CEM/VLB0.45, CEM/VLB5, and CEM/VLB10 cells, stained with Coomassie blue. A total of 10 μg of membrane proteins was deposited in each lane. MW: molecular weight marker. (B) Immunolabeling of P-gp with the C219 monoclonal antibody after electrotransfer onto nitrocellulose of the proteins from the gel in panel A. Conditions are described in Materials and Methods. (C) Control in the absence of the primary antibody in resistant cell lines, as indicated, in the conditions described in panel B. Arrowheads indicate the migration of Pgp.

Table 1: Amino acid Sequences and Analysis of Peptides Identified by Mass Spectrometry

peptide sequence	length	position
YMVFR	5	790
GNLEFR	6	390
NLEEAKR	7	280
IIGVFTR	7	735
LNVQWLR	7	1104
QFFHAIMR	8	150
GAAYEIFK	8	360
FDTLVGER	8	520
TTIVIAHR	8	581
RLNVQWLR	8	1103
TCIVIAHR	8	1226
KQFFHAIMR	9	149
TVIAFGGQK	9	263
SGHKPDNIK	9	381
NVHFSYPSR	9	396
STTVQLMQR	9	434
YMVFRSMLR	9	790
STVVQLLER	9	1077
VVSQEEIVR	9	1139
NVHFSYPSRK	10	396
EANAYDFIMK	10	506
QDVSWFDDPK	10	799
IATEAIENFR	10	896
KPTVSVFSMFR	11	31
LPHKFDTLVGER	12	516
EKKPTVSVFSMFR	13	29
AGAVAEEVLAAIR	13	250
IIDNKPSIDSYSK	13	368
VGDKGTQLSGGQK	13	1169
EALDESIPPVSFWR	14	686
FEHMYAQSLQVPYR	14	916
EANIHAFIESLPNK	14	1151
VKEHGTHQQLLAQK	14	1251
GIYFSMVSVQAGTK	14	1265
ILSSFTDKELLAYAK	15	235
NADVIAGFDDGVIVEK	16	594
QEIGWFDVHDVGELNTR	17	158
VQSGQTVALVGNSGCGK	17	417
LYDPTEGMVSVDGQDIR	17	443
LSTIQNADLIVVFQNGR	17	1234
QDVSWFDDPKNTTGALTTR	19	799
EIIGVVSQEPVLFATTIAENIR	22	468
TVVSLTQEQKFEHMYAQSLQVPYR	24	906
ILLLDEATSALDTESEAVVQVALDK	25	551
AHLGIVSQEPILFDCSIAENIAYGDNSR	28	1111

We first showed that cholesterol depletion with MβCD did not change the apparent amount of P-gp in the membrane extracts, as shown in Figure 4A, strongly suggesting that P-gp is not significantly extracted from the membrane by the depletion procedure.

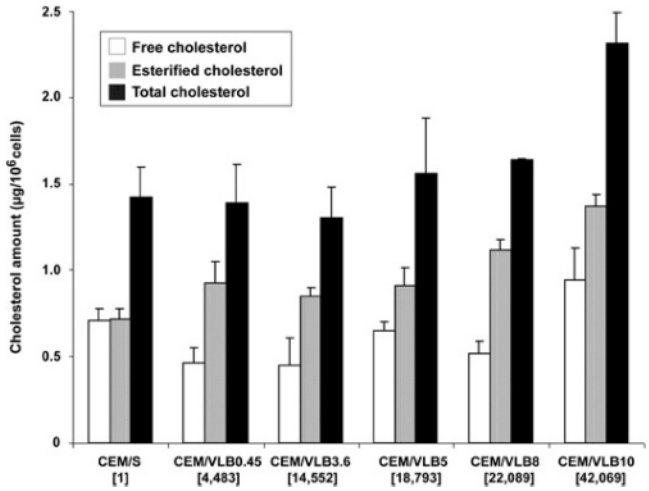

FIGURE 3: Total (black bars), free (white bars), and esterified (gray bars) cholesterol contents of various CEM cell lines. The amount of total cholesterol is measured as described in Materials and Methods from sensitive CEM/S and resistant CEM/VLB0.45, CEM/VLB3.6, CEM/VLB5, CEM/VLB8, and CEM/VLB10 cells, as indicated. Results are the average of five independent tests with standard deviation ($p < 0.025$). Values between brackets represent the index of resistance, which was measured according to a previously published method (*18*).

We observed that the apparent surface area A_0 corresponding to the onset of nonzero surface pressure was of 750, 1000, and 1250 cm^2/mg membrane proteins for monolayers resulting from CEM/S, CEM/VLB0.45, and CEM/VLB10 cells, respectively (Figure 4B), indicating that the A_0 value increased with the level of chemoresistance of the cell lines.

In addition, using the same set of membrane preparation, we observed that the A_0 surface area obtained with membrane monolayers from untreated (control) and depleted CEM/VLB0.45 cells decreased linearly with the decrease of membrane cholesterol (Figure 4C). This result suggests that the membrane organization is strictly correlated with the amount of cholesterol in the monolayers. It is interesting to note that when the cholesterol of depleted CEM/VLB0.45 membranes reached the amount of 0.040 mg/mg of membrane proteins, which is equivalent to the level of cholesterol of nontreated sensitive CEM/S cells (0.039 mg/mg $\pm$ 0.005 ($n = 3$)), the A_0 surface area (750 cm^2/mg of membrane

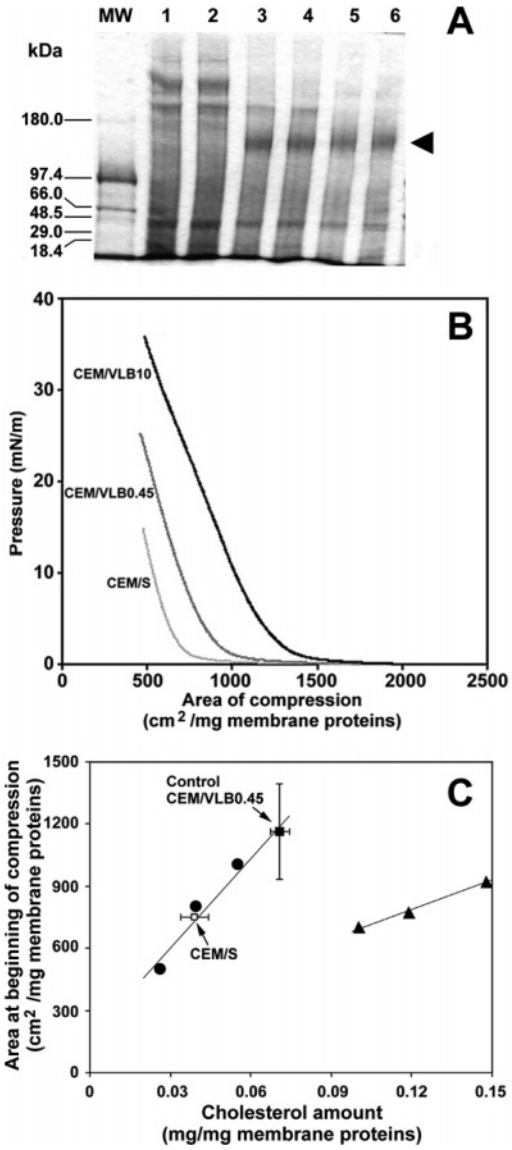

FIGURE 4: Effect of cholesterol depletion by MβCD on cell membranes. (A) 8% SDS−PAGE of membrane extracts from sensitive CEM/S (lanes 1 and 2) and resistant CEM/VLB0.45 (lanes 3 and 4) and CEM/VLB10 (lanes 5 and 6) cells before (lanes 1, 3, 5) and after (lanes 2, 4, 6) cholesterol depletion with 1.5 mM MβCD. MW: molecular weight marker. Proteins (10 μg per lane) were deposited and migrated as described in Materials and Methods. The gel slab was stained with Coomassie Blue. (B) Compression of membrane monolayers from sensitive CEM/S and resistant CEM/VLB0.45 and CEM/VLB10 cells analyzed by the Langmuir technique. Membrane monolayers were prepared by depositing membrane fractions, corresponding to 80 μg of membrane proteins. One typical experiment is presented; experimental variation in the isotherms is less than 3%. (C) A_0 surface areas of membrane monolayers from untreated (control CEM/VLB0.45, black square, mean of two independent experiments); cholesterol-depleted by addition of 0.3, 0.6, or 1.5 mM MβCD (black circles, three independent results); and repleted (black triangles, three independent results) CEM/VLB0.45 cells by addition of 0.3 μL/mL MβCD/cholesterol complex. The open square represents the A_0 surface area for CEM/S cells, which contains 0.039 ± 0.005 mg cholesterol/mg membrane proteins (mean of three independent results). Membrane monolayers were prepared as described above. The A_0 surface area is obtained from the compression isotherms presented in panel B.

proteins) was very similar to that of the sensitive cells (800 cm^2/mg of membrane proteins). Moreover, we showed that the area at the beginning of compression obtained with monolayers from repleted CEM/VLB0.45 cells that had been previously depleted was also linearly correlated to the amount of membrane cholesterol. However, these values are not superimposable on the values obtained from membranes that do not contain added cholesterol. This last result strongly suggests that added cholesterol did not insert into the monolayer in the same manner as cholesterol that is naturally present in the membranes does.

ATPase Activity of P-gp as a Function of the Amount of Membrane Total Cholesterol in CEM Cells. It has been reported that the P-gp ATPase activity appears to increase in the presence of cholesterol in reconstituted membranes (*9*, *12*). In our cellular model, we observed that the amount of membrane cholesterol increased from the IR of CEM/VLB5 cells (18 700) (Figure 3), while the maximal amount of P-gp that membranes of resistant cells could hold reached a plateau from that IR (Figure 1). Since P-gp was the sole ABC transporter involved in the MDR phenotype of CEM, we investigated whether the cholesterol content could influence the activities of P-gp in membranes at the cellular level. Therefore, cell membranes were depleted and repleted using MβCD in the presence of mevalonate and lovastatin. The measured cholesterol amount in the fetal bovine serum used to culture the cells was 0.36 ± 0.01 mg/mL and dropped down to 0 mg/mL after depletion with the Cab-O-Sil resin. Additionally, the amounts of cholesterol in CEM/S, CEM/VLB0.45, and CEM/VLB10 cells were measured before any treatment, after cholesterol depletion, and after cholesterol repletion of previously cholesterol-depleted cells.

In the absence of any treatment, the ATPase activities were 283 ± 41 nmol/min/mg of proteins and 450 ± 46 nmol/min/mg of proteins for CEM/VLB0.45 and CEM/VLB10, respectively, as indicated in Figure 5. The main ATPase activity of total membrane extracts measured in the presence of a cocktail of non-P-gp ATPase activities was mainly devoted to P-gp (as we have previously shown (*17*)). After 45% membrane cholesterol depletion, the ATPase activity decreased to 127 and 170 nmol/min/mg of proteins, which represent 45 and 38% of the initial activity, respectively. By contrast, 2-fold cholesterol enrichment induced a 2-fold increase in the ATPase activity (i.e., 514 nmol/min/mg of proteins and 1101 nmol/min/mg of proteins for CEM/VLB0.45 and CEM/VLB10 cells, respectively). These results suggest that the ATPase activity correlates with the amount of membrane cholesterol in a linear relationship. In addition, a statistical *t*-test on the means showed that the slopes of the regression lines obtained from both cells lines were identical ($p > 0.05$). Therefore, whatever the chemoresistance level, the presence of cholesterol is essential to the ATPase activity of P-gp.

This conclusion could be corroborated by the repletion of cholesterol in the membranes of both CEM/VLB0.45 and CEM/VLB10 cell lines. Figure 6 shows that when 55.9 and 41.5% of the total cholesterol contents were withdrawn from the membrane, the ATPase activity decreased by 54.8 and 51.6% of the initial activity in CEM/VLB0.45 and CEM/VLB10 cells, respectively, whereas cholesterol repletion up to 80.9% of the initial value in both cell types raised the ATPase activity to 96.4 and 87.4% of the initial activity in CEM/VLB0.45 and CEM/VLB10 cells, respectively. These results demonstrate that the P-gp ATPase activity depends on the amount of membrane cholesterol and may be almost

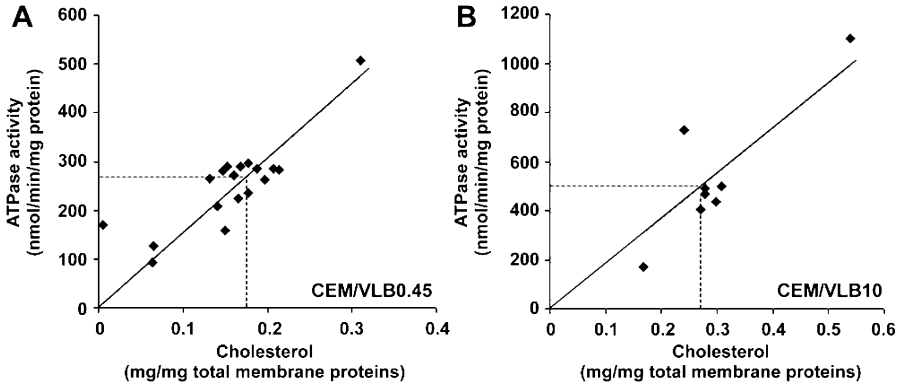

FIGURE 5: ATPase activity of P-gp as a function of the amount of total cholesterol present in the membranes of CEM/VLB0.45 (A) and CEM/VLB10 (B) cells. Membrane extracts from CEM/VLB0.45, CEM/VLB10, and CEM/S (for control) cells were depleted of their cholesterol with MβCD whose concentration varied from 0 to 1.5 mM, as described in Materials and Methods. The ATPase activity is expressed in nmol of ATP hydrolyzed per min and per mg of membrane proteins. Cholesterol was measured by the cholesterol oxidase method. Dotted lines indicate the mean values for nontreated cells. Data are the result of 18 (A) and eight (B) independent measurements. Regression lines take all the measurements into account and were extrapolated to zero.

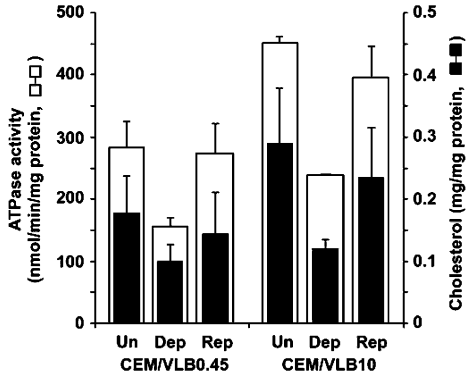

FIGURE 6: Reversibility of the cholesterol-induced activation of the P-gp ATPase activity. Membranes of CEM/VLB0.45 and CEM/VLB10 cells were prepared as indicated in Materials and Methods. The ATPase activity of P-gp was measured by the fluorimetric method described in Materials and Methods. The left scale corresponds to the ATPase activity (open bars), and the right scale corresponds to the amount of total cholesterol per mg of total membrane proteins (solid bars). Measurements were carried out on control (Un) and cholesterol-depleted (Dep) membrane extracts, and in cholesterol-repleted (Rep) membrane extracts that had been previously depleted of their cholesterol, from CEM/VLB0.45 and CEM/VLB10 cells as indicated. Values are averages of two independent measurements ± standard deviation.

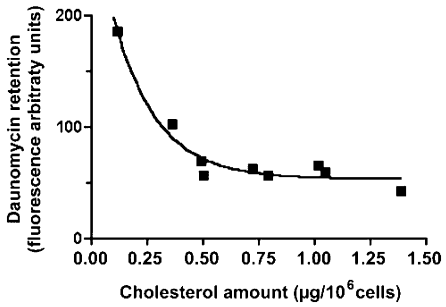

FIGURE 7: Intracellular retention of daunomycin as a function of the amount of total cholesterol in CEM/VLB0.45 cells. Cells were depleted of their cholesterol with 0−1.5 mM MβCD. Cells (0.5×10^6/mL) in exponential growth phase were incubated with 1.9 μM daunomycin for 3 h at 37 °C and then washed twice in PBS prior to their analysis by flow cytometry as described in Materials and Methods. Amounts of cell cholesterol were determined in parallel of each cytometry assay. Values in the ordinate correspond to the average cellular fluorescence of daunomycin. Each measurement results from the analysis of 10 000 cells. Nine independent experiments were carried out.

completely reversed to its initial value after cholesterol repletion of previously depleted cells.

P-gp-Mediated Drug Efflux as a Function of the Amount of Membrane Total Cholesterol in CEM Cells. Since membrane cholesterol activates the ATPase activity of P-gp, we considered whether it, also, affects the function of transport of drugs by P-gp. To test this hypothesis, we measured by flow cytometry the retention of daunomycin in CEM/VLB0.45 that had been gradually depleted of their membrane cholesterol. We observed that the lower the membrane total cholesterol level was, the higher the level of intracellular retention of daunomycin, according to an exponential decay curve (Figure 7). Thus, in our model, when membrane cholesterol was decreased 11.6 times (to carry it to 0.12 μg/10^6 cells), the retention of daunomycin increased 4.4 times. In addition, Figure 8 shows that after either CEM/VLB0.45 or CEM/VLB10 cells had been depleted of their membrane cholesterol, which induced an increased intracellular retention of daunomycin, repletion of cholesterol in the membranes by 0.3 μL/mL methyl-β-cyclodextrin/cholesterol complex slightly decreased the retention of daunomycin without retrieving the initial values (a *t*- test to compare means of daunomycin retention after cholesterol depletion and after cholesterol repletion showed that means were significantly different for a probability $\alpha < 0.02$ and $\alpha < 0.001$, respectively, for CEM/VLB0.45 and CEM/VLB10 cells). The same test was carried out with control sensitive CEM/S cells and showed no significant difference between the retention of daunomycin measured by the median of the fluorescence peak of intact, depleted, and repleted cells incubated with daunomycin (results not shown).

The results reported in Table 2 show that initial membrane cholesterol amounts were not significantly different in CEM/S and CEM/VLB0.45 cells, while they were 1.6 times lower than in CEM/VLB10 cells. Moreover, after depletion of 60, 38, and 36% of membrane cholesterol from CEM/S, CEM/VLB0.45, and CEM/VLB10 cells, respectively, subsequent cholesterol repletion replenished at least 92% of the initial amount of cholesterol.

In conclusion, these results show that cholesterol depletion favors the intracellular retention of daunomycin. They also show that cholesterol replenishment of previously cholesterol-

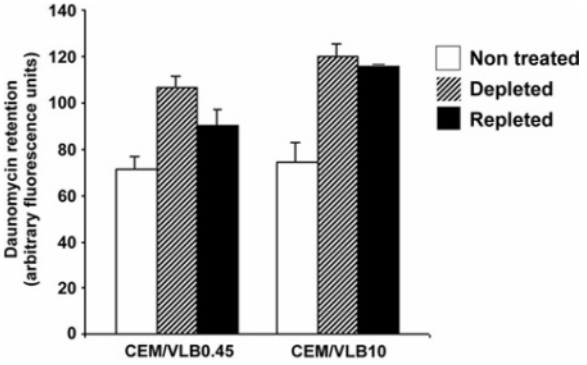

FIGURE 8: Cholesterol-related reversibility of the intracellular retention of daunomycin in CEM/VLB0.45 and CEM/VLB10 cells. Conditions are described in the legend to Figure 7. Nontreated (white bars), cholesterol-depleted (1.5 mM MβCD, slashed bars), and cholesterol-repleted (0.3 μL/mL MβCD/cholesterol complex, black bars) from CEM/VLB0.45 and CEM/VLB10 cell lines were washed twice in PBS prior to their analysis by flow cytometry. Daunomycin (1.9 μM) was then added to the cell culture, which was treated as described above. Data are the average of two independent measurements with standard deviations. Cell cholesterol amounts are given in Table 2.

Table 2: Total Cholesterol Contents in the Sensitive CEM/S and the Resistant CEM/VLB0.45 and CEM/VLB10 Cells[a]

	CEM/S	CEM/VLB0.45	CEM/VLB10
initial	1.42 ± 0.20	1.39 ± 0.23	2.28 ± 0.21
depleted	0.86 ± 0.23	0.53 ± 0.17	0.83 ± 0.10
repleted	1.32 ± 0.30	1.36 ± 0.24	2.10 ± 0.25

[a] Cell total cholesterol was measured as described in Materials and Methods and is given in μg/10^6 cells. Cells were either intact, depleted of their membrane cholesterol, or repleted after a previous depletion. Results are mean of two independent experiments ± standard deviation.

depleted cells does not allow the complete restoration of daunomycin retention to its initial values, while P-gp ATPase activity had reached its initial value.

Chemosensitization as a Function of the Amount of Membrane Total Cholesterol in CEM Cells. Since cholesterol depletion and repletion lead to reversible effects of both P-gp ATPase activity and retention of daunomycin, we evaluated the influence that variations of membrane cholesterol could have on the apoptosis of resistant CEM cells. A viability test performed prior to the flow cytometry analysis showed that 90−95% of the cells were alive at the time of analysis. The flow cytometry experiments, shown in Figure 9, reveal that cholesterol depletion to the same extent as that reached in Figure 8 induced apoptosis of more than 40% of the CEM/VLB0.45 cell population (panel B), when compared to control cells (panel A). This was mainly due to the intracellular accumulation of daunomycin since cholesterol depletion of CEM/VLB0.45 cells in the absence of daunomycin revealed no induction of apoptosis (not shown). In addition, complete reversibility of this phenomenon was obtained after cholesterol repletion of previously depleted CEM/VLB0.45 cells (panel C).

DISCUSSION

In this paper, we report that membrane cholesterol is a central element for the control of both ATPase and drug transport activities of P-glycoprotein and is closely related to the level of expression of the typical multidrug resistance phenotype of cancer cells.

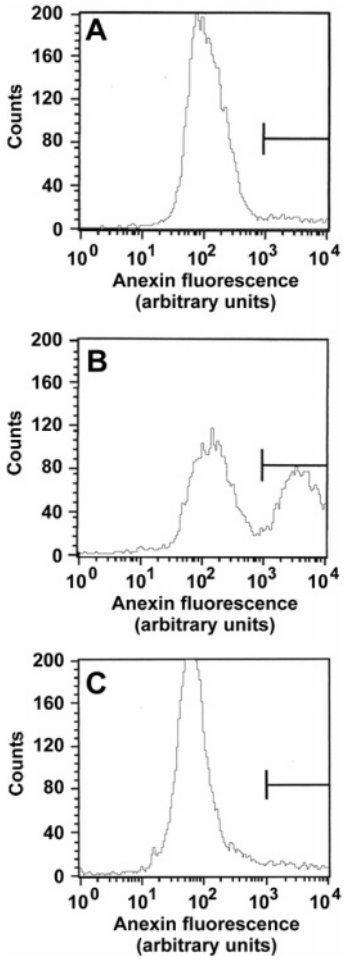

FIGURE 9: Chemosensitization to daunomycin of cholesterol-depleted CEM/VLB0.45 cells. Cells (0.5×10^6) in exponential growth phase were depleted of their membrane cholesterol using 1.5 mM MβCD according to the protocol described in Materials and Methods. They were subsequently incubated with 1.9 μM daunomycin for 3 h and then washed twice in PBS prior to the addition of anexin V-FLUOS. Analysis by flow cytometry was carried out according to the anexin V-FLUOS kit recommendations. Sensitization to daunomycin was determined by measurement of the fluorescence of anexin V-FLUOS. Each peak collected the fluorescence of 8000 cells. (A) Control CEM/VLB0.45 cells in the presence of 1.9 μM daunomycin. (B) Cholesterol-depleted CEM/VLB0.45 cells (1.5 mM MβCD) in the presence of 1.9 μM daunomycin. (C) Cholesterol-repleted (0.3 μL/mL MβCD/cholesterol complex) CEM/VLB0.45 cells that had been previously depleted, in the presence of 1.9 μM daunomycin.

CEM leukemia cells display a resistance to both vinblastine and daunomycin, which are known to be extruded by both P-gp and MRP1 proteins. Our results showed that P-gp is the sole protein responsible for the typical MDR phenotype of these resistant CEM cells. The pattern of expression of the *MDR*1 mRNA follows that of the production of P-gp in all the resistant CEM cell lines studied, suggesting that the increase in the level of chemoresistance is due to the overexpression of P-gp and thereby enhancement of drug efflux by P-gp.

Role of Cholesterol on the Membrane Organization. A previous study of membranes of resistant and nonresistant CEM cells by electron microscopy revealed an increase in the number of 6−9 nm diameter particles at the level of the membranes of CEMVLB4500 cells (cultured in the presence of 4.5 μg/mL vinblastine) (*7*). This feature could be attributed

to a proteolipidic reorganization of the membranes, but this work was unable to specify whether the particles corresponded to proteins or more complex structures. We approached the problem of the proteolipidic organization of the membrane using Langmuir compression isotherms, to study membrane monolayers from sensitive and resistant CEM cells. Our results show that the proteolipidic organization of the membranes of chemoresistant CEM cells differs from that of their parental sensitive CEM/S cells and changes with the level of chemoresistance. More particularly, the increase in the A_0 surface area correlates with the increased level of chemoresistance, indicating that the proteolipidic reorganization of the membrane in relation with the MDR phenotype varies in the sense of a tight organization. To prove that the main actor of such phenomenon was cholesterol, we analyzed the effect of its depletion from CEM/VLB0.45 membranes. Thus, when the remaining amount of cholesterol was equivalent to that of sensitive cells (0.04 mg/mg of membrane proteins), the A_0 surface area (800 cm^2/mg of membrane proteins) corresponds to that of sensitive CEM/S membranes. Since the latter are devoid of P-gp, we can exclude P-gp in the process of the proteolipid reorganization of membrane monolayers and strongly suggest that in this context cholesterol plays the major role. However, in a lipid bilayer, P-gp-mediated lipid translocation from one leaflet to the other is able to cause perturbation in the organization of bilayer constituents, whereas cholesterol imparts stability to this perturbation of the bilayer organization by P-gp (*12*).

P-gp may be indirectly involved in the organization of membranes through cholesterol homeostasis. Indeed, the involvement of P-gp in the process of cholesterol esterification has been described in support of the physiological function for P-gp in facilitating cholesterol trafficking; the molecular mechanism of the latter is dissociated from the conventional drug transport activity of P-gp (*6*). In contrast, the same authors showed that in polarized cells, enhanced cholesterol esterification is observed in mice deficient in *mdr*1a and *mdr*1b P-glycoproteins (*30*). In CEM cells, which are not polarized, we showed that enhancement of membrane cholesterol with the level of the MDR phenotype mainly concerned esterified cholesterol.

Cholesterol Modulates P-gp Activities in Different Ways. P-gp ATPase activity is linearly activated by increasing amounts of cholesterol, and repletion of membrane cholesterol in cells that had been previously depleted of their cholesterol restores the initial P-gp ATPase activity. In addition, the linear relationship that links the P-gp ATPase activity to the amount of membrane cholesterol in both CEM/VLB0.45 and CEM/VLB10 cells (Figure 5) shows that the two regressions share the same slope, suggesting that cholesterol offers the same type of membrane microenvironment to P-gp in both cell lines presenting highly different levels of resistance.

The P-gp drug transport activity is also activated by increasing amount of cholesterol but in a nonlinear manner, and after repletion, the level of drug efflux activity remains always lower than the initial value.

Our results show that the P-gp ATPase and drug transport activities depend on the amount of membrane cholesterol. The decreased P-gp activity resulting from cholesterol depletion could be explained by differential P-gp expression and/or localization. However, it is known that P-gp is a relatively stable protein with a half-life of 14−17 h (*31*). In addition, (i) the cholesterol modulation experiments we carried out never exceeded 8 h and (ii) no MβCD-induced pull out effect on P-gp could be observed while cholesterol was depleted from the membrane (Figure 4A). The approach that we used does not make it possible to determine the localization of the P-gp in the membrane microdomains but rather comprehend the membrane as a whole. Our results indicate that the cholesterol depletion led to a disruption of the membrane, which could not be restored completely after repletion since the transport activity of P-gp does not regain its initial level. This contrasts with recent results according to which cholesterol repletion allowed P-gp to be relocated in rafts while it retrieved the totality of its transport activity (*32*). This difference can possibly be explained by the level of cholesterol depletion that, in our case, is likely to have strongly disorganized any initial raft structure, without, however, having pulled P-gp off the membrane. It is, however, probable that cholesterol depletion destroyed the rafts thus leading P-gp to be located in nonraft zones of the membrane. This is in agreement with the repletion results described in Figure 4C, which strongly suggest that the depletion of cholesterol destroys the membrane microstructure that contains P-gp and that cannot be restored by a subsequent cholesterol repletion. These results suggest that the effect of cholesterol modulates P-gp activities in different ways. Therefore, we propose that cholesterol exerts a direct effect on the ATPase activity of P-gp, while acting on the transport activity via the structuring of the membrane, which depends on cholesterol redistribution after repletion.

All together, these results strongly suggest that cholesterol is involved in the P-gp-induced MDR phenotype and controls both ATPase and drug efflux activities of P-gp.

Effects of Cholesterol and Other Lipids on Chemosensitization of Resistant CEM Cells. It is interesting to note that when the membrane cholesterol decreased, the retention of daunomycin was enhanced in a nonlinear manner (Figure 7), which reflects a complex relationship between cholesterol and drug retention in resistant cells. This phenomenon of daunomycin retention was observed whatever the level of chemoresistance (i.e., CEM/VLB0.45 and CEM/VLB10).

After cholesterol repletion to obtain about the amount as that present in nontreated cells, daunomycin retention remained elevated and never regained the initial value. This phenomenon may be due to a modification of the structure of P-gp induced by the modification of the membrane organization (cf. *Langmuir Isotherm Experiments*). Since the initial membrane organization cannot be reconstituted by subsequent cholesterol repletion, we can suppose that (i) the partition coefficient of daunomycin is different, thereby modifying its transport properties through the membrane and (ii) the P-gp/lipid interactions are modified thereby rendering P-gp inapt for its drug extrusion activity.

The fact that P-gp ATPase activity can be recovered to about its initial value after cholesterol repletion suggests that the P-gp ATPase and transport activities have been uncoupled.

We observed that cholesterol depletion provoked an important level of apoptosis of CEM resistant cells due to the intracellular accumulation of daunomycin, which was able to reach its target. This phenomenon was totally

reversible since cells recovered their initial viability after cholesterol repletion.

Since the depletion of cholesterol does not restore the drug transport activity of P-gp, the daunomycin retained should lead to cell mortality; thus, it is probable that the disturbance caused by cholesterol leads daunomycin to be retained in areas where it has no action on its target. For example, it can be imagined that because of the uncoupling between ATPase and drug transport activities, daunomycin would remain trapped in the membrane and/or on the level of P-gp, which explains the reversibility of apoptosis.

After cholesterol repletion, we observed that the retention of daunomycin was higher in the cells with a high level of resistance (CEM/VLB10) as compared to those of lower resistance (CEM/VLB0.45) (cf. Figure 8). In the first case, the organization of the membrane is tighter so that reorganization is more difficult to restore after repletion of cholesterol. Moreover, CEM/VLB10 cells contain a higher amount of P-gp, strongly suggesting that daunomycin has tendency to accumulate more specifically on the level of P-gp.

Our results propose the central role of cholesterol in maintaining the MDR phenotype. Nevertheless, other lipids, and particularly lipids involved in raft and caveolae formation, could also be implicated in MDR. It has been observed that glucosylceramide contents increase with the expression of the MDR phenotype (*33*). Moreover, it has been shown by the use of antisense DNA to knock out the glucosylceramide synthase gene that affected cells are 28-fold less chemoresistant than native cells (*34*). In addition, glucosylceramide appears to be a substrate of P-gp (*4*). All these results suggest the implication of glucosylceramide in chemoresistance. Sphingomyelin will be also a good candidate to play a role in the P-gp-dependent MDR phenotype, due to its very important affinity and vicinity to cholesterol (*35*) and because it appears to be a substrate of P-gp (*4*).

Our results open new ways toward the therapy of cancer chemoresistance. Thus, the discovery of new means to change the proteolipid organization of the membrane of chemoresistant cells to that corresponding to chemosensitive cells may make it possible to effectively modulate the typical MDR phenotype knowing that, in this case, the reduction in the amount of membrane cholesterol leads to chemosensitization.

The results also allow a improved understanding of why several ABC transporters are more particularly localized in membrane regions enriched in cholesterol. These regions could involve DRMs and caveolae since cholesterol and P-gp are largely present in these membrane domains.

As we have shown in CEM cells, the variation of membrane cholesterol content in cells that express the MDR phenotype could depend on the level of chemoresistance.

ACKNOWLEDGMENT

We are grateful to Mrs. Jeanine Bernaud for her help with the flow cytometry technique and to Dr. Michel Becchi for the MALDI-TOF analysis.

REFERENCES

1. Bates, S. E. (2003) Solving the problem of multidrug resistance: ABC transporters in clinical oncology, in *ABC proteins From Bacteria to Man*, pp 359−390, Academic Press, New York.
2. Scala, S., Akhmed, N., Rao, U. S., Paull, K., Lan, L. B., Dickstein, B., Lee, J. S., Elgemeie, G. H., Stein, W. D., and Bates, S. E. (1997) P-glycoprotein substrates and antagonists cluster into two distinct groups, *Mol. Pharmacol. 51*, 1024−1033.
3. Sparreboom, A., Danesi, R., Ando, Y., Chan, J., and Figg, W. D. (2003) Pharmacogenomics of ABC transporters and its role in cancer chemotherapy, *Drug Resist. Update 6*, 71−84.
4. van Helvoort, A., Smith, A. J., Sprong, H., Fritzsche, I., Schinkel, A. H., Borst, P., and van Meer, G. (1996) MDR1 P-glycoprotein is a lipid translocase of broad specificity, while MDR3 P-glycoprotein specifically translocates phosphatidylcholine, *Cell 87*, 507−517.
5. Debry, P., Nash, E. A., Neklason, D. W., and Metherall, J. E. (1997) Role of multidrug resistance P-glycoproteins in cholesterol esterification, *J. Biol. Chem. 272*, 1026−1031.
6. Luker, G. D., Nilsson, K. R., Covey, D. F., and Piwnica-Worms, D. (1999) Multidrug resistance (MDR1) P-glycoprotein enhances esterification of plasma membrane cholesterol, *J. Biol. Chem. 274*, 6979−6991.
7. Arsenault, A. L., Ling, V., and Kartner, N. (1988) Altered plasma membrane ultrastructure in multidrug-resistant cells, *Biochim. Biophys. Acta 938*, 315−321.
8. Garcia-Segura, L. M., Ferragut, J. A., Ferrer-Montiel, A. V., Escriba, P. V., and Gonzalez-Ros, J. M. (1990) Ultrastructural alterations in plasma membranes from drug-resistant P388 murine leukemia cells, *Biochim. Biophys. Acta 1029*, 191−195.
9. Urbatsch, I. L., and Senior, A. E. (1995) Effects of lipids on ATPase activity of purified Chinese hamster P-glycoprotein, *Arch. Biochem. Biophys. 316*, 135−140.
10. May, G. L., Wright, L. C., Dyne, M., Mackinnon, W. B., Fox, R. M., and Mountford, C. E. (1988) Plasma membrane lipid composition of vinblastine sensitive and resistant human leukaemic lymphoblasts, *Int. J. Cancer 42*, 728−733.
11. Pallares-Trujillo, J., Domenech, C., Grau-Oliete, M. R., and Rivera-Fillat, M. P. (1993) Role of cell cholesterol in modulating vincristine uptake and resistance, *Int. J. Cancer 55*, 667−671.
12. Rothnie, A., Theron, D., Soceneantu, L., Martin, C., Traikia, M., Berridge, G., Higgins, C. F., Devaux, P. F., and Callaghan, R. (2001) The importance of cholesterol in maintenance of P-glycoprotein activity and its membrane perturbing influence, *Eur. Biophys. J. 30*, 430−442.
13. Troost, J., Albermann, N., Emil Haefeli, W., and Weiss, J. (2004) Cholesterol modulates P-glycoprotein activity in human peripheral blood mononuclear cells, *Biochem. Biophys. Res. Commun. 316*, 705−711.
14. Hinrichs, J. W., Klappe, K., Hummel, I., and Kok, J. W. (2003) ABC transporters are enriched in noncaveolar DIGs in human multidrug resistant cancer cells, *J. Biol. Chem. 279*, 5734−5738.
15. Bendayan, R., Lee, G., and Bendayan, M. (2002) Functional expression and localization of P-glycoprotein at the blood brain barrier, *Microsc. Res. Technol. 57*, 365−380.
16. Garrigues, A., Escargueil, A. E., and Orlowski, S. (2002) The multidrug transporter, P-glycoprotein, actively mediates cholesterol redistribution in the cell membrane, *Proc. Natl. Acad. Sci. U.S.A. 99*, 10347−10352.
17. Dong, M., Penin, F., and Baggetto, L. G. (1996) Efficient purification and reconstitution of P-glycoprotein for functional and structural studies, *J. Biol. Chem. 271*, 28875−28883.
18. Baggetto, L. G., Dong, M., Bernaud, J., Espinosa, L., Rigal, D., Bonvallet, R., and Marthinet, E. (1998) In vitro and in vivo reversal of cancer cell multidrug resistance by the semisynthetic antibiotic tiamulin, *Biochem. Pharmacol. 56*, 1219−1228.
19. Heider, J. G., and Boyett, R. L. (1978) The picomole determination of free and total cholesterol in cells in culture, *J. Lipid. Res. 19*, 514−518.
20. Gray, M. C., Plant, A. L., Nicholson, J. M., and May, W. E. (1995) Microenzymatic fluorescence assay for serum cholesterol, *Anal. Biochem. 224*, 286−292.
21. Nakamura, M., Kondo, H., Shimada, Y., Waheed, A. A., and Ohno-Iwashita, Y. (2003) Cellular aging-dependent decrease in cholesterol in membrane microdomains of human diploid fibroblasts, *Exp. Cell. Res. 290*, 381−390.
22. Kilsdonk, E. P., Yancey, P. G., Stoudt, G. W., Bangerter, F. W., Johnson, W. J., Phillips, M. C., and Rothblat, G. H. (1995) Cellular cholesterol efflux mediated by cyclodextrins, *J. Biol. Chem. 270*, 17250−17256.
23. Weinstein, D. B. (1979) A single-step adsorption method for removal of lipoproteins and preparation of cholesterol-free serum, *Circulation 59* Suppl. II, 54.

24. Phalen, T., and Kielian, M. (1991) Cholesterol is required for infection by Semliki Forest virus, *J. Cell. Biol. 112*, 615−623.
25. Marquardt, M. T., and Kielian, M. (1996) Cholesterol-depleted cells that are relatively permissive for Semliki Forest virus infection, *Virology 224*, 198−205.
26. Dong, M., Baggetto, L. G., Falson, P., Le Maire, M., and Penin, F. (1997) Complete removal and exchange of sodium dodecyl sulfate bound to soluble and membrane proteins and restoration of their activities, using ceramic hydroxyapatite chromatography, *Anal. Biochem. 247*, 333−341.
27. Bradford, M. M. (1976) A rapid and sensitive method for the quantitation of microgram quantities of protein utilizing the principle of protein−dye binding, *Anal. Biochem. 72*, 248−254.
28. Laemmli, U. K. (1970) Cleavage of structural proteins during the assembly of the head of bacteriophage T4, *Nature 227*, 680−685.
29. Zaitsev, S., Volchenkova, T. A., Ustinova, O. A., Koshtigo, T. V., Baggetto, L. G., Fleury, F., Madoulet, S., Nabiev, I. R., and Oleinikov, V. A. (2002) Study of P-glycoprotein effect on the lipid monolayer properties by the Langmuir−Blodgett technique, *Biofizika 47*, 1073−1079.
30. Luker, G. D., Dahlheimer, J. L., Ostlund, R. E., Jr., and Piwnica-Worms, D. (2001) Decreased hepatic accumulation and enhanced esterification of cholesterol in mice deficient mdr1a and mdr1b P-glycoproteins, *J. Lipid Res. 42*, 1389−1394.
31. Muller, C., Laurent, G., and Ling, V. (1995) P-glycoprotein stability is affected by serum deprivation and high cell density in multidrug-resistant cells, *J. Cell. Physiol. 163*, 538−544.
32. Troost, J., Lindenmaier, H., Haefeli, W. E., and Weiss, J. (2004) Modulation of cellular cholesterol alters P-glycoprotein activity in multidrug resistant cells, *Mol. Pharmacol. 66*, 1332−1339.
33. Lavie, Y., Cao, H., Bursten, S. L., Giuliano, A. E., and Cabot, M. C. (1996) Accumulation of glucosylceramides in multidrug-resistant cancer cells, *J. Biol. Chem. 271*, 19530−19536.
34. Liu, Y. Y., Han, T. Y., Giuliano, A. E., Hansen, N., and Cabot, M. C. (2000) Uncoupling ceramide glycosylation by transfection of glucosylceramide synthase antisense reverses adriamycin resistance, *J. Biol. Chem. 275*, 7138−7143.
35. Wattenberg, B. W., and Silbert, D. F. (1983) Sterol partitioning among intracellular membranes. Testing a model for cellular sterol distribution, *J. Biol. Chem. 258*, 2284−2289.

BI048669W